Determination of pore size distribution and hydraulic properties using nuclear magnetic resonance relaxometry: A comparative study of laboratory methods

L. R. Stingaciu, L. Weihermüller, S. Haber-Pohlmeier, S. Stapf, H. Vereecken, and A. Pohlmeier

Received 25 September 2009; revised 28 June 2010; accepted 12 July 2010; published 3 November 2010.

[1] In this study, we evaluate the feasibility of using nuclear magnetic resonance (NMR) relaxometry measurements to characterize pore size distribution and hydraulic properties in four porous samples with different texture and composition. We compare NMR with two classical techniques based on water retention and mercury intrusion measurements. Both T_2 and T_1 NMR relaxation measurements at 6.47 MHz were carried out for three saturated model samples (medium sand, fine sand, and a homogenous sand/kaolin clay mixture) and one saturated natural silt loam soil. Cumulative pore size distribution functions and mean pore diameters were calculated assuming average surface relaxivity parameters and a cylindrical capillary model of the pores. The mean pore diameters derived from T_2 and T_1 distributions as well as the cumulative pore size distribution functions agree satisfactorily with those derived from mercury intrusion and retention curves. The observed deviations are due to limitations of each method, sample preparation, and sample composition. To evaluate the influence of the variations observed in the hydraulic properties of the samples, the pore size distribution functions were scaled back to water retention functions, and the van Genuchten hydraulic parameters were estimated by inversion using the RETC software. The comparison shows that both T_2 and T_1 NMR relaxation measurements can be used to estimate pore size distribution and mean pore diameter, as well as the retention function and corresponding hydraulic properties.

Citation: Stingaciu, L. R., L. Weihermüller, S. Haber-Pohlmeier, S. Stapf, H. Vereecken, and A. Pohlmeier (2010), Determination of pore size distribution and hydraulic properties using nuclear magnetic resonance relaxometry: A comparative study of laboratory methods, *Water Resour. Res.*, 46, W11510, doi:10.1029/2009WR008686.

1. Introduction

[2] Understanding water, liquid, and solute flow is a key issue in a wide range of applications such as agriculture, forestry, ecology, and civil engineering and also in more technical areas like exploration and material sciences. In general, the physical parameters of porous media are routinely determined to characterize the material and parameterize predictive models. Most commonly, porosity, surface area, permeability, wettability, and grain size are measured while the pore size distribution is mainly determined indirectly from water retention (release) curves. The measurement of the retention curve using either the combination of porous plate and pressure cell or multistep outflow is tedious, expensive, and time consuming. Furthermore, the results could be biased as a consequence of sample prepa-

Copyright 2010 by the American Geophysical Union. 0043-1397/10/2009WR008686

W11510 1 of 11

ration [Weihermüller et al., 2009; Bittelli and Flury, 2009]. As an alternative for quick and reliable pore size distribution, and therefore retention curve determination, nuclear magnetic resonance (NMR) measurements can be successfully used. It is well known that the amplitude of the proton NMR signal is proportional to the fluid content and that relaxation times give information on the pore size distribution. Over the last few years, new NMR methodologies and applications have been developed and tested to quantify the total amounts of fluid phase, fluid saturation, and porosity distributions in porous media [Kleinberg and Horsfield, 1990; Latour et al., 1995; Hinedi et al., 1997; Barrie, 2000; Schaumann et al., 2005]. In general, NMR measurements are extensively used by the oil industry (well logging) to estimate and quantify hydrocarbon in reservoirs and the rate at which they can be economically extracted [Hedberg et al., 1993; Kleinberg, 1994, 1996; Straley et al., 1997]. In soil science, NMR measurements can be used successfully to quantify and estimate the amount of water in soils [Votrubová et al., 2000; Pohlmeier et al., 2009; Stingaciu et al., 2009] and its spatial variability, and to observe the infiltration and distribution of different types of solutes in soils [Amin et al., 1996; Van As and van Dusschoten, 1997; Oswald et al., 1997; Herrmann et al., 2002; Pohlmeier et al., 2008]. All these processes and state variables are dominated by the

¹Agrosphere Institute, ICG-4, Forschungszentrum Jülich, Jülich, Germany.

²Macromolecular Chemistry Department, RWTH Aachen University, Aachen, Germany.

³Department of Technical Physics II, Ilmenau University of Technology, Ilmenau, Germany.

hydraulic properties of the observed media which are usually derived from water retention curves. In the simplest assumption on the geometrical representation of a given porous medium, the water retention characteristics can be extracted from pore size distribution on the basis of an empirical law that relates the pore suction to the effective pore radius. Prior work has shown that the pore size distributions of sand and soils can be successfully derived from T_1 NMR relaxometry field-cycling measurements when surface relaxivity parameters are calculated on the basis of the average relaxation time and surface-to-volume ratio available from additional Brunauer-Emmett-Teller (BET) measurements [Pohlmeier et al., 2009]. Other recently published research involved a study in which the pore size distribution of a number of natural soils was determined from T2 NMR relaxometry measurements following two approaches. The first used one average surface relaxivity parameter, and the second used two surface relaxivity parameters: one for large pores and one for small pores derived at two different water saturations [Jaeger et al.,

- [3] The detection of NMR signal in natural soils can be significantly reduced when the relaxation is accelerated by the presence of paramagnetic impurities such as Fe^{3+} and Mn^{2+} ions [Hall et al., 1997; Keating and Knight, 2007]. At all solid-liquid interfaces, magnetic susceptibility differences cause local magnetic field gradients, which influence the transversal relaxation process, leading to additional relaxation caused by the diffusion of water in these gradients. Since the magnitudes of these effects depend on the strength of the main magnetic field B_0 and echo spacing T_E , they should diminish with decreasing magnetic field strength and for sufficiently short T_E . Furthermore, assuming a homogenous distribution of the paramagnetic centers, the average surface relaxivity parameters will be increased and approximately correct pore sizes can be obtained.
- [4] Our goal is to assess the usefulness of both T_2 and T_1 NMR relaxometry for the determination of pore size distribution and hydraulic properties of natural porous media in comparison to classical soil physics laboratory methods. T_2 and T_1 low-field NMR relaxation measurements were performed on four different porous media with increasing complexity and heterogeneity. The results were compared in terms of cumulative pore size distribution functions (PSD- T_2 and PSD- T_1) with those derived from classically determined water retention characteristics (PSD-pF) and mercury intrusion porosimetry measurements (PSD-Hg). The hydraulic properties of the materials were estimated further from the pore size distributions and compared in order to analyze how the deviations between the obtained cumulative pore size distribution functions influence the hydraulic properties of the investigated porous media.

2. Materials and Methods

2.1. Soil Samples

[5] Four different soil samples were used in the study, whereby three samples were artificial substrates: medium sand (FH31) with a grain size distribution between 0.72 mm and 0.18 mm, Milisil fine sand (W3), and a mixture (Mix8) of FH31 and 8% mass percentage of kaolin clay (FH31 and W3 were provided by Quarzwerke Frechen, Germany; kaolin clay was provided by Sigma-Aldrich, Germany). In

addition, a natural soil from Merzenhausen, Germany (MZ) (50°54′N, 6°24′E) was used. The Merzenhausen soil was characterized as an Orthic Luvisol, horizon A, containing 80% w/w silt and 18% w/w clay [Kasteel et al., 2007]. For NMR measurements and the determination of the water retention curve (with the exception of the MZ sample for which the retention curve was determined for an undisturbed soil column), the samples were homogenized, sieved, and packed at the same packing density. For mercury intrusion porosimetry, both sieved and conglomerate structures were used.

2.2. Nuclear Magnetic Resonance (NMR)

[6] Generally, the NMR signal intensity of a spin-echo experiment can be written as

$$SI \propto N(H) \left(e^{-T_{\rm E}/T_2} \right) \left(1 - e^{-T_{\rm R}/T_1} \right)$$
 (1)

where N(H) is the proton density, $T_{\rm E}$ is known as echo time, and $T_{\rm R}$ is repetition time, the last two being varied appropriately during the experiment. T_2 is the spin-spin relaxation time and T_1 is the spin-lattice relaxation time, both of which are physical properties of the fluid. The relaxation times were related to the dimension of the pores by the Brownstein-Tarr equation [Brownstein and Tarr, 1977, 1979]:

$$\frac{1}{T_{1,2}} = \frac{1}{T_{1,2B}} + \rho_{1,2} \cdot \frac{S}{V} + \left(\frac{1}{T_{2D}}\right) \tag{2}$$

where $T_{1;2B}$ are the relaxation times of bulk water, ρ_1 and ρ_2 are the surface relaxivity parameters for longitudinal and transversal relaxation, and SV^{-1} is the pore-surface-topore-volume ratio. The last term in equation (2) is the relaxation induced by diffusion in internal magnetic field gradients; it is added to the equation for T_2 only, since it is known that diffusion only affects transverse relaxation and not longitudinal relaxation. From equation (2), T_1 and T_2 measurements can be used to determine surface relaxivity parameters if information about the surface-to-volume ratio, S/V, is known from additional independent measurements of the specific surface area by BET (adsorption of gas molecules on a solid surface) [Brunauer et al., 1938]. In our study, the average S/V ratios were derived from a specific surface area determined by nitrogen adsorption, with exception of the FH31 sample. In this case, it was determined by the provider. Each surface relaxivity parameter was assumed to be constant for a given sample and controlled by the surface properties of the pore walls. Assuming cylindrical pores with diameter D and neglecting the diffusion term for transverse relaxation, the pore diameter can be calculated by

$$\frac{1}{T_{1;2}} = \frac{1}{T_{1;2B}} + \rho_{1;2} \cdot \frac{4}{D}.$$
 (3)

[7] In our study, H-NMR relaxometry measurements were performed on saturated samples in order to determine the transversal and longitudinal relaxation times and were performed on the soil solutions extracted by centrifugation to characterize bulk relaxation. The substrates were filled into glass tubes with an inner diameter of 24 mm and a height of 46 mm. The experiments were conducted on a Halbach magnet with a magnetic field strength of 0.15 T

Table 1. Hydraulic Properties for the Four Substrates FH31, W3, Mix8, and Merzenhausen Soil (MZ)^a

Sample	Method	Bulk Density (g/cm ³)	$\theta_{\rm r}^{\rm b}$ (cm ³ /cm ³)	$\theta_{\rm s}$ (cm ³ /cm ³)	$\alpha \ (\mathrm{cm}^{-1})$	n
FH31	pressure plates	1.58	0.020	0.321	0.0330	5.40
W3	MSO	1.42	0.058	0.333	0.0089	2.78
Mix8	Rosetta	1.45	0.061	0.410	0.0036	2.66
MZ	pressure plates	1.60	0	0.438	0.0071	1.21

^aParameters of FH31 and MZ are based on pressure plate measurements. W3 was determined using multistep outflow (MSO) and Mix8 using ROSETTA software [*Schaap et al.*, 2001].

[Raich and Blümler, 2004] that was connected to a STELAR spectrometer (Stelar, Mede, Italy). The resonator was a solenoid RF coil with an inner diameter of 4 cm and length of 6 cm. For the determination of T_2 relaxation time, the Carr-Purcell-Meiboom-Gill (CPMG) pulse sequence was employed [Carr and Purcell, 1954; Meiboom and Gill, 1958]:

90° RF pulse $-(T_{\rm E}/2 - 180^{\circ} \text{ RF pulse} - T_{\rm E}/2 - \text{echo acquisition})_n$

with n = 15,000 echoes and $T_{\rm E} = 150~\mu \rm s$. For the determination of T_1 relaxation time, the IR-CPMG (inversion recovery CPMG) pulse sequence was used:

 180° RF inversion pulse $-\tau-90^{\circ}$ RF pulse - FID acquisition,

where FID is free induction decay. Value τ was varied in 32 logarithmically spaced steps between 4 \cdot $T_{1\text{max}}$ and $0.01 \cdot T_{1\text{max}}$ ms.

2.3. Mercury Intrusion Porosimetry

[8] The mercury porosimetry method characterizes the porosity of the observed material by applying various levels of pressure to a sample immersed in mercury. Assuming cylindrical capillary pore geometry, the Washburn equation [*Washburn*, 1921] relates the pore diameter to the applied pressure of mercury by

$$D_i = \frac{-4 \cdot \sigma_{\text{Hg}} \cdot \cos \gamma_{\text{Hg}}}{P_i} \tag{4}$$

where D_i is the diameter, $\sigma_{\rm Hg}$ is the surface tension of Hg, $\gamma_{\rm Hg}$ is the contact angle of Hg, and P_i is mercury pressure. The system used in our measurements is a standard porosimeter. The sample is placed into a container that is evacuated to remove contaminant gases and vapors. While still evacuated, mercury is allowed to fill the container. Next, pressure is increased in small steps, and the volume of mercury is measured after each intrusion equilibration. The volume of mercury intruding into the sample because of an increase in pressure from P_i to P_{i+1} is proportional to the volume of pores in the associated size range D_i to D_{i+1} as shown by Washburn's equation [Webb, 2001].

[9] The sandy samples FH31 and W3 were loaded in the penetrometer and packed at the same packing density as for the NMR measurements. The Mix8 and MZ samples were used as solid conglomerates. A pressure between 4.82 kPa and 31.7 MPa was applied as this pressure would force mercury into pores between 400 and 0.05 μ m in diameter [*Micromeritics*, 2010].

2.4. Water Retention Curves

[10] The water retention curves were determined using the standard sand bed/pressure cell or multistep outflow method. Only for the Mix8 sample were no measured retention curve data available. Therefore, a pedotransfer function implemented in ROSETTA [Schaap et al., 2001] was used to predict the hydraulic properties in this case. For the parameterization of the water retention curves, the Mualemvan Genuchten approach [Mualem, 1976; van Genuchten, 1980] was used, whereby the effective volumetric water content S_e is defined as

$$S_{e} = \frac{\theta - \theta_{r}}{\theta_{s} - \theta_{r}} \begin{cases} 1 & h \ge 0 \\ (1 + |\alpha h|^{n})^{-m} & h < 0, \quad \alpha, m > 0 \quad n > 1 \end{cases}$$
 (5)

where $\theta_{\rm r}$ and $\theta_{\rm s}$ (cm³/cm³) are the residual and saturated volumetric water contents; α (cm⁻¹), n (–), and m (–) (m=1-1/n) are shape parameters. The hydraulic properties of the reference materials, as well as the measurement source are summarized in Table 1.

[11] In general, retention curves are usually interpreted as cumulative distribution functions in comparison to pore size distribution functions which are mostly plotted as a function of frequency. Using the retention characteristic, pore size distribution can be extracted for a given porous medium on the basis of an empirical law that relates the pore suction to the effective pore radius. Many models have been developed for this purpose. *D'Hollander* [1979] proposed a probabilistic model based on lognormal pore size distribution; *Kosugi* [1994, 1996] used a lognormal distribution model; *Vogel* [2000] introduced a network model; *Tuller et al.* [1999] and *Tuller and Or* [2001] used a dual continuum pore space representation model.

[12] Nevertheless, these models will not simplify the comparison of PSD-pF curves with the PSD-NMR and PSD-Hg curves, as is the case with the assumption made in our study, since the cylindrical capillary model assumed is commonly used for the evaluation of these measurements. Therefore, according to *Jury and Horton* [2004], the pore system was assumed to be a bundle of cylindrical capillary tubes with a random distribution of radii; the capillary pressure could then be related to the pore dimension according to the Young-Laplace equation:

$$h = \frac{2\sigma\cos\gamma}{rg\rho} \tag{6}$$

where h is the pressure head or capillary rise, σ is the surface tension, γ is the contact angle between liquid and solid

^bFor better correlation between the measurements in further calculations, θ_r was set to 0.

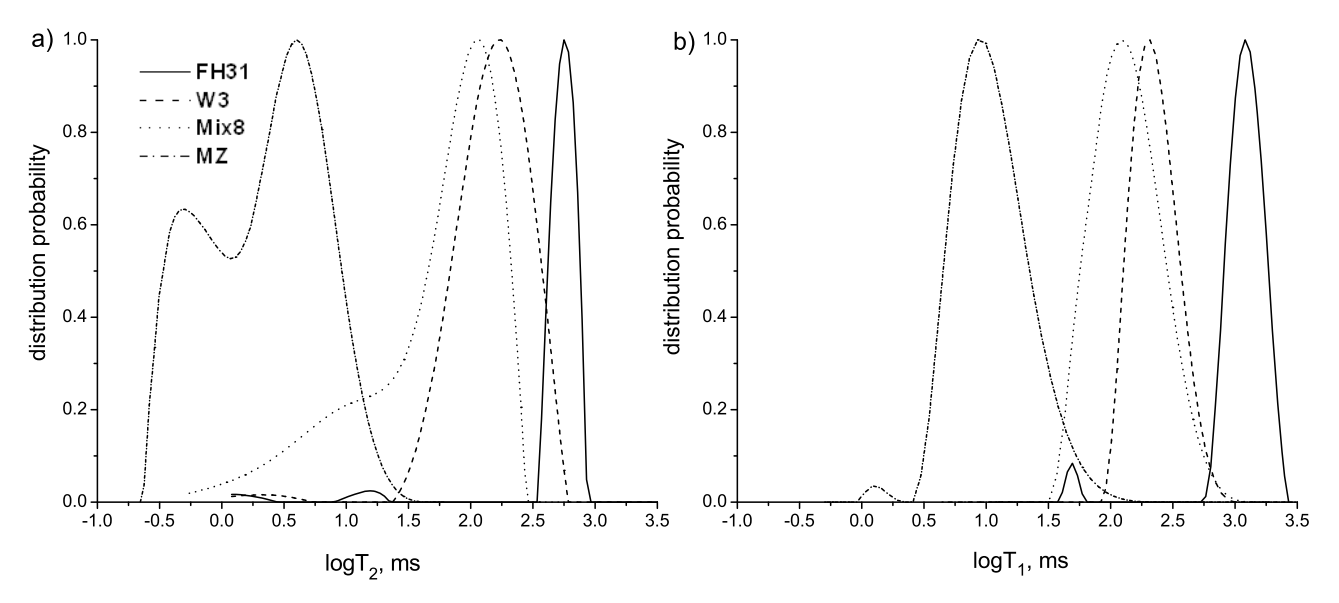


Figure 1. (a) T_2 and (b) T_1 relaxation time distribution functions for the four substrates FH31, W3, Mix8, and MZ.

phase, r is the pore radius, g is the standard gravity, and ρ is the fluid density.

3. Results and Discussions

3.1. NMR Results

[13] The transversal relaxation time, T_2 , distribution functions obtained using inverse Laplace transformation [Song et al., 2002] are plotted for each of the four samples in Figure 1a. The T_2 relaxation distribution functions are monomodal for sandy samples FH31 and W3, with an average relaxation time of 560 ms for FH31 and 162 ms for W3. The Mix8 and MZ samples present wide (over three orders of magnitude) bimodal T_2 relaxation distribution functions, with average values of 47 ms for Mix8 and 0.69 ms for MZ. The natural soil sample, MZ, relaxes very quickly in comparison to all other samples. The relaxation could be enhanced by the magnetic susceptibility of some of the soil components. Figure 1b shows the longitudinal relaxation time, T_1 , distribution functions for each sample. The distributions can be described as monomodal for all samples with average relaxation times of 1200 ms for FH31, 213 ms for W3, 125 ms for Mix8, and 10 ms for the MZ sample, whereby the MZ sample shows a wide distribution that smears out to longer T_1 values and masks a possible relaxation mode at about 60 ms.

[14] Instead of analyzing only the classical T_1 and T_2 relaxation distribution functions as plotted in Figure 1, cumulative

pore size distributions functions were calculated according to equation (3). Average surface relaxivity parameters $\rho_{1,2}$ were estimated for each sample according to equation (2). The surface-to-volume ratios (S/V) were supplied from BET measurements, and the bulk relaxation times were measured for each soil solution extracted from samples by centrifugation. The surface relaxivity parameters ρ_1 and ρ_2 , bulk relaxation times, S/V ratios, and the obtained average pore diameters for all samples are listed in Table 2. Typically, rocks and soils have a ρ_2/ρ_1 ratio, which is generally equal to T_1/T_2 , namely between 1 and 3 (1 < T_1/T_2 < 3). In our case the following ρ_2/ρ_1 ratios were determined: 2.93 for FH31, 1.33 for W3, 2.91 for Mix8, and 4.6 for the MZ sample. For the W3 and Mix8 samples, both ρ_2 and ρ_1 values were in the expected range (around 3 μ m/s [Kleinberg, 1999]). For the FH31 sample, even though the ρ_2/ρ_1 ratio had a reasonable value (2.93), the individual surface relaxivity parameters were quite large. This could point to an error in estimating the S/V ratio. Since we were not able to determine the specific surface using BET for this medium sand (the specific area was too small for the BET technique in our laboratory), its value used in the calculation of S/V was taken from producer information. The S/V ratio depends on the packing procedure, which may create differences between the information provided by the producer and the actual sample used in our study. The large ρ_2/ρ_1 value for the MZ sample could be due to the diffusion in internal magnetic field gradients. It is well known that

Table 2. Calculated Surface Relaxivity Parameters and Average Pore Diameters From NMR Relaxation Measurements

Sample	ρ_2 , Surface Relaxivity $(\mu \text{m/s})$	ρ_1 , Surface Relaxivity $(\mu m/s)$	T _{2B} (ms)	T _{1B} (ms)	Specific Area (cm ² /g)	S/V (cm ⁻¹)	D _{2av} (μm)	D _{1av} (μm)
FH31	47	16	2280	2786	68	381	140	135
W3	3.6	2.7	1683	2279	3600	19108	2.6	2.5
Mix8	3.5	1.2	1012	1469	15950	60823	0.7	0.7
MZ	12	2.7	578	787	96440	327918	0.1	0.1

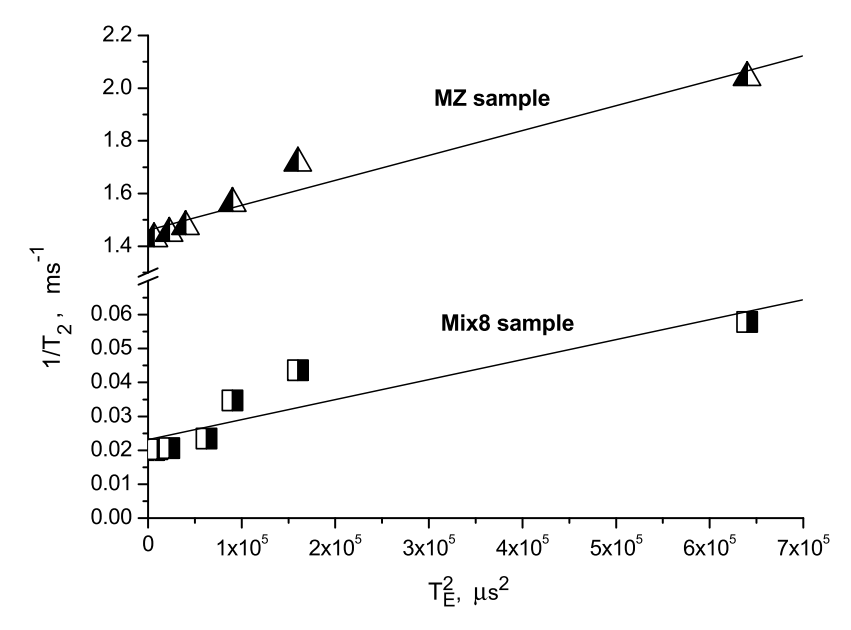


Figure 2. Estimation of diffusion influence: $1/T_{2,average}$ as a function of T_E^2 for the two fine samples Mix8 and MZ.

diffusion will affect the T_2 distribution and that diffusion effects are enhanced in fine grain materials [Kleinberg, 1999]. Therefore, the influence of diffusion was checked for the two fine samples Mix8 and MZ by varying the echo spacing in the CPMG train and observing the shift of the distribution functions. Figure 2 shows the average relaxation rates, $1/T_2$, as a function of T_E^2 . For the Mix8 sample, weak acceleration due to diffusion in internal gradients was observed for small T_E values (80, 100, and 150 μ s). This has also been sustained by a previous study [Stingaciu et al., 2009] showing that for a magnetic field strength of 0.1 T, the choice of $T_E = 150~\mu$ s for a similar sand/clay sample produces no truncated information and that the diffusion effects are minimized. This allows us to neglect diffusion in

equation (2). For the MZ sample, a steeper gradient was observed; nevertheless, for lower $T_{\rm E}$ values (80, 150, and 200 μ s), the $1/T_2$ data obtained with these settings were very close to those extrapolated to $T_{\rm E}=0$, so that the influence of diffusion in residual field gradients is minimal and cannot be the cause of the observed variations. As a result, diffusion can again be neglected in further evaluations of pore diameter. It should be noted that larger deviations occurred with increasing echo time.

[15] From the relaxation time distribution functions, the cumulative pore size distribution functions were calculated by scaling equation (2) with the average surface relaxivities ρ_2 and ρ_1 , respectively. The normalized cumulative pore size distributions functions are displayed in Figure 3, where

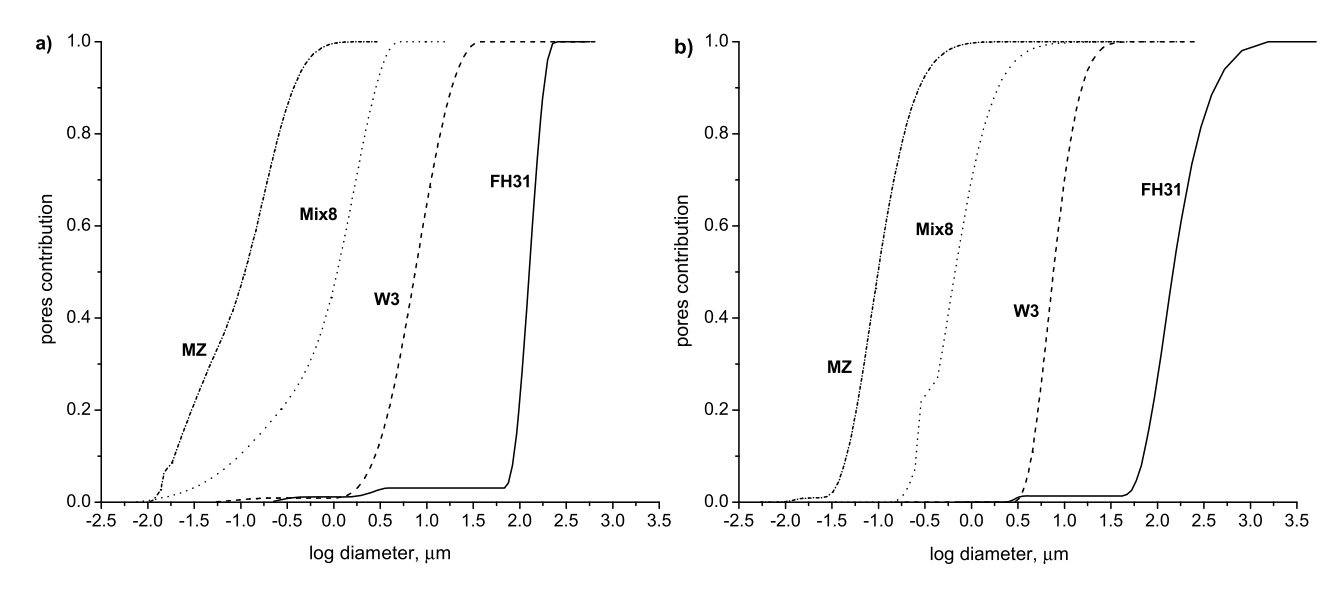


Figure 3. Cumulative pore size distribution calculated according to equation (3). (a) PSD- T_2 and (b) PSD- T_1 for the four substrates FH31, W3, Mix8, and MZ.

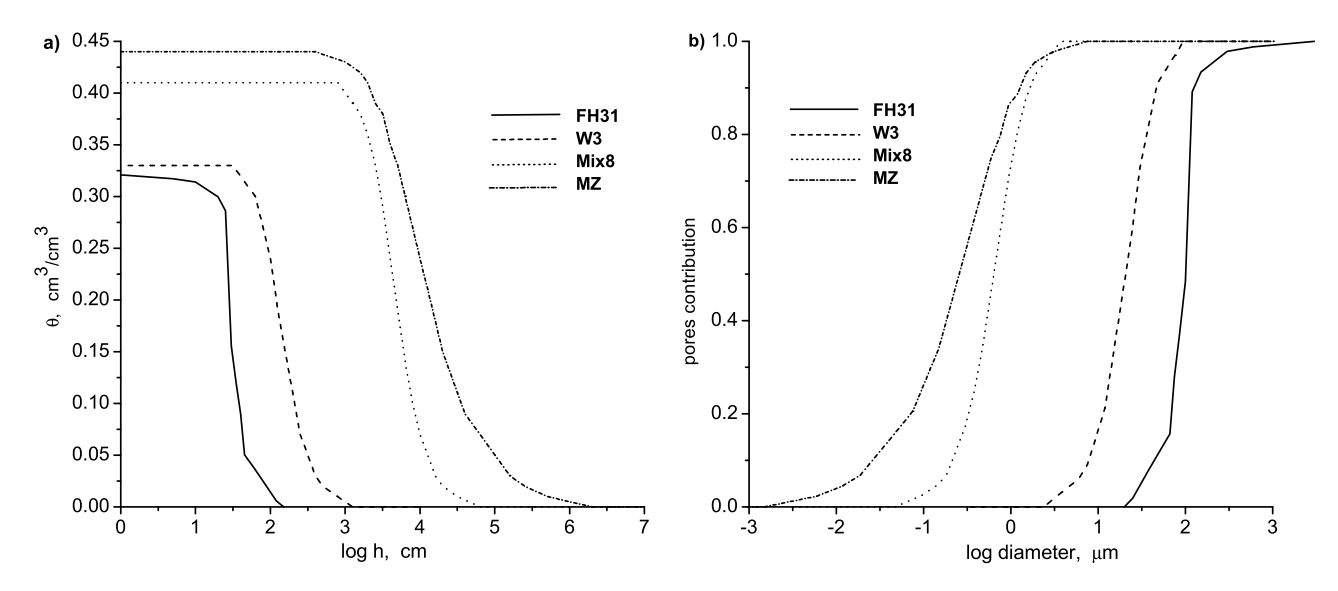


Figure 4. (a) Water retention curves for the three artificial substrates (FH31, W3, and Mix8) and the natural soil Merzenhausen (MZ). FH31 and MZ are based on pressure plate measurements; W3 was determined using multistep outflow (MSO) and Mix8 was determined using ROSETTA [*Schaap et al.*, 2001] pedotransfer function. (b) Normalized pore size diameter functions based on the retention curves using equation (6).

1 is the sum of all pore sizes equivalent to 100%. In general, the pore size distributions obtained from T_2 measurements (PSD- T_2 , see Figure 3a) indicate a narrow distribution of pores for the sandy samples FH31 and W3 with values ranging between 30 and 300 μ m for FH31 and between 0.3 and 10 μ m for W3. This is in good agreement with the results of Pohlmeier et al. [2009], who found a mean pore size of around 150 μ m for a similar FH31 sample. A larger spectrum of pore sizes was obtained for Mix8 and MZ samples with values ranging from 0.007 to 3 μ m for Mix8 and 0.01 to 0.7 μm for MZ. These values are a result of the mix of fine and coarse grains within the samples. Figure 3b shows the pore size distributions obtained from T_1 measurements (PSD- T_1). Again, the well-sorted sandy materials W3 and FH31 indicate a narrow pore size distribution. For fine samples with medium and high clay content, like our Mix8 and MZ samples, the BET method measures a specific surface that is rather controlled by the surface area of the clay particles and not by the surface of pores. The relaxivity parameters based on the calculation of such surface areas have low values (a few micrometers per second) and represent in most cases the relaxivity of clay-bound water, i.e., water in the interlayer spaces of clay packets [Kleinberg, 1999], which has a long exchange time with the surrounding bulk water. This does not provide information on the water in the pores (pore dimensions). On the other hand, dispersed clay particles in the pores would accelerate bulk relaxation even if the water on the surface of clay exchanges efficiently with pore water. Therefore the PSD- T_1 and PSD- T_2 of such materials can be a poor estimator of the real pore size distribution.

3.2. Retention Functions Results

[16] The water retention curves plotted in Figure 4a are based on different sources such as multistep outflow (MSO) (W3), pressure cells (FH31 and MZ), and the use of a pedotransfer function (Mix8). The pressure head as plotted

in the abscissa (Figure 4a) was transformed into pore diameter using the Young-Laplace equation (equation (6)), as described in section 2. In addition, the ordinate was normalized to 1 (100%) corresponding to full saturation θ_s . The pore size distributions obtained (PSD-pF) are displayed in Figure 4b. It can be seen that the pore sizes are narrowly distributed for the well-sorted sandy samples FH31 and W3. In contrast, Mix8 and MZ show a wider pore spectrum. From these curves, the mean pore diameter can be easily estimated. For FH31, W3, Mix8, and MZ, the mean pore diameters are 98.90, 20.41, 0.64, and 0.25 μ m, respectively.

3.3. Mercury Intrusion Results

[17] The pore size distributions from mercury intrusion measurements (PSD-Hg) were also obtained as cumulative functions in which the equivalent pore diameter was cal-

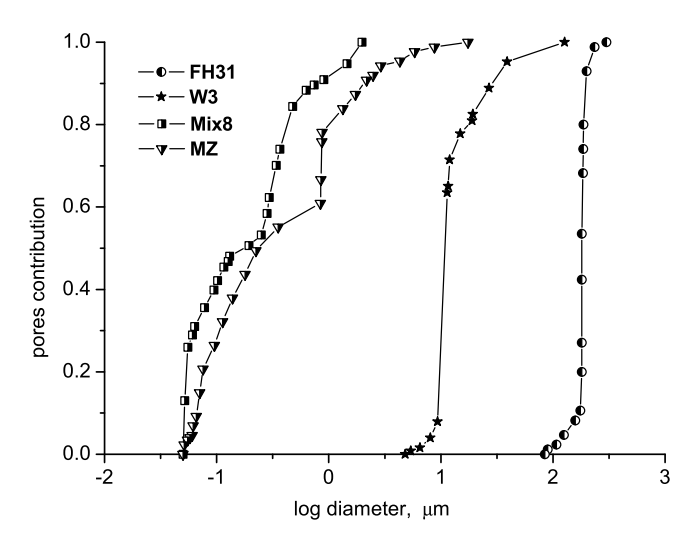


Figure 5. Cumulative pore size distribution based on mercury intrusion (PSD-Hg) for all four soil samples.

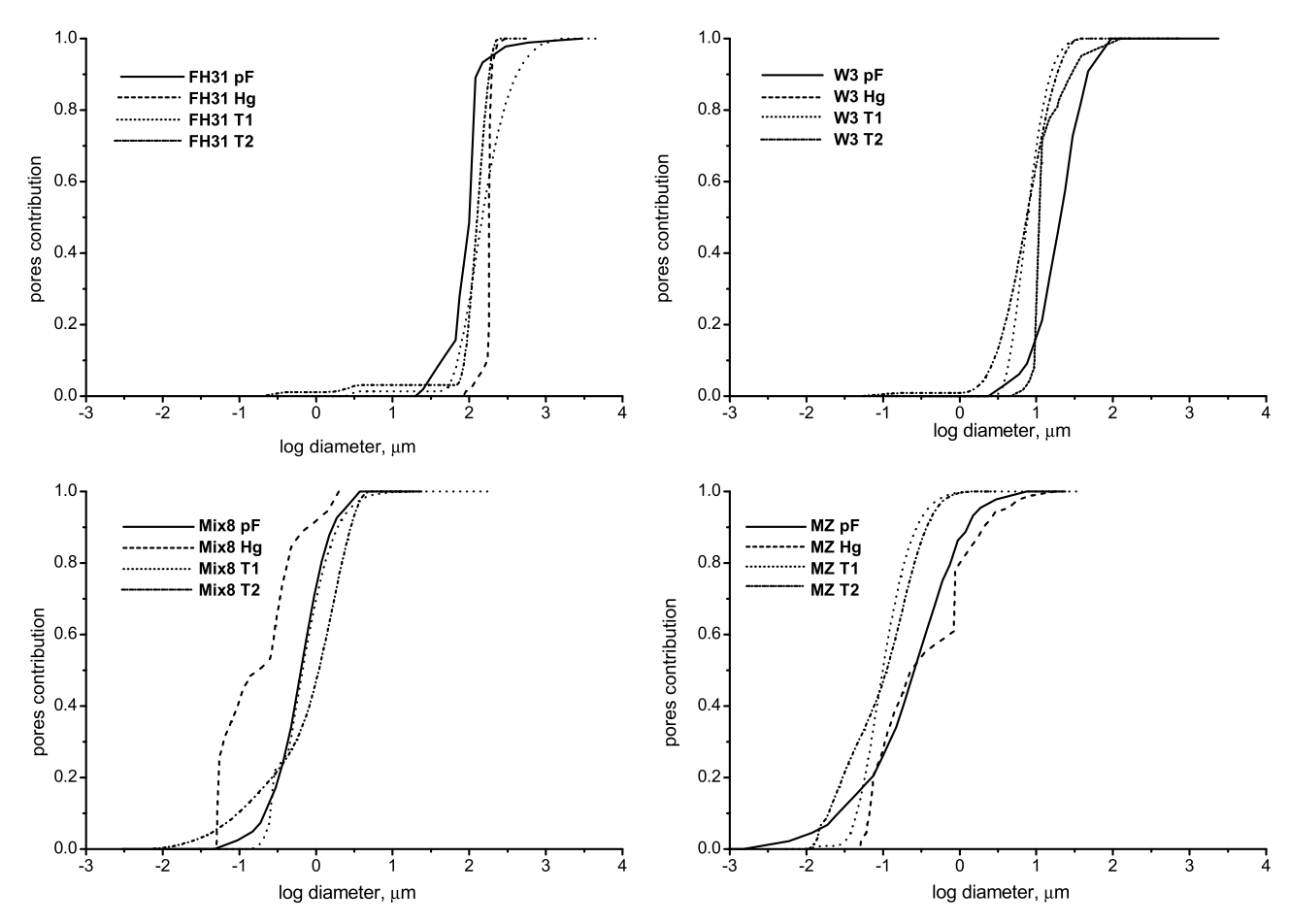


Figure 6. Cumulative pore size distribution (PSD) functions for all measurements and for all four samples.

culated according to equation (4) from experimental data collected for a various number of mercury pressure steps. The cumulative distribution functions are presented in Figure 5. They show a monomodal distribution of pores for the FH31 and W3 samples with average pore diameters of 178 μ m for FH31 and 10 μ m for W3. The distributions indicate that more than 80% of the total volume corresponds to pores with a diameter smaller than 180 μ m in the case of the FH31 sample and less than 18 μ m in the case of W3 sample. The pore diameter distributions for the MZ and Mix8 samples show wide multimodal distributions with average values of 0.22 μ m for MZ and 0.17 μ m for Mix8, respectively. Nevertheless, 80% of the pore volume of Mix8 is below 0.40 μ m, and 80% of MZ is below 1 μ m.

3.4. Comparison of the Different Measurements

[18] For a better comparison of all three methods used for PSD determination, the calculated average pore diameters are presented in Table 3 together with some assumed uncertainty ranges estimated from the following sources: (1) for the NMR-derived average diameters, the uncertainty is assumed to be in a 10% interval, as previously shown by *Stingaciu et al.* [2009]; (2) for the retention function derived diameters, the uncertainty is assumed to be in a 70% interval as *Bittelli and Flury* [2009] have shown in their work; and (3) lacking a realistic experimental estimation of the errors that can occur in Hg intrusion measurements, the errors were

assumed to be maximal, e.g., 50%, as suggested in a technical note from Micromeritics [2010]. The average pore diameters obtained from all measurements are in the same order of magnitude for each of the four samples used for investigation. Nevertheless, some differences can be observed in the mean pore diameter obtained from the pF function in comparison with the mean pore diameters obtained from the other measurements for the well-sorted sandy samples FH31 and W3. The MZ and Mix8 average diameters obtained from NMR relaxation measurements and mercury intrusion are slightly smaller than the diameters derived from the retention curve (pF). Possible reasons for these differences will be discussed below. To gain a better understanding of the mismatch observed in the mean pore diameters, we display the cumulative PSD functions from all measurements in Figure 6. In the fol-

Table 3. Average Pore Diameter for All Samples Together With Their Specific Uncertainty Interval^a

Sample	D_{av} -Hg (μ m)	D_{av} - $T_2~(\mu\mathrm{m})$	D_{av} - $T_{1}~(\mu\mathrm{m})$	D_{av} -p (μ m)
FH31	177.82 ± 85	140 ± 14	135 ± 13.5	98.90 ± 70
W3	10.71 ± 5	2.6 ± 0.26	2.5 ± 0.25	20.41 ± 14
Mix8	0.17 ± 0.09	0.7 ± 0.07	0.7 ± 0.07	0.64 ± 0.42
MZ	0.22 ± 0.11	0.1 ± 0.01	0.1 ± 0.01	0.25 ± 0.14

^aSamples calculated according to equation (3) for T_1 and T_2 NMR relaxation measurements, equation (4) for Hg intrusion, and equation (6) for water retention function.

lowing, the discussion of the obtained results is conducted as a comparison of methods with respect to the type of sample used for investigation.

[19] The NMR T_1 and T_2 relaxation measurements provide nearly identical distributions of the pore diameters for all samples where the average values coincide systematically because of the ρ_2 and ρ_1 constants. The less steep function of T_2 indicates a slight overestimation of the larger pores as well as an overestimation of smaller pores, especially for the two fine samples Mix8 and MZ. These differences could be partially due to the fact that relaxation in inhomogeneous fields leads to a signal decay that is generally nonexponential with an initial decay rate, which is a weighted sum of T_1 and T₂ relaxation times, as Hürlimann and Griffin [2000] and Chelcea et al. [2009] have suggested. However, in a Halbach magnet, the magnetic field gradients are more on the grain scale, and the overall variation of the B_0 and B_1 fields is not large enough to produce the effect described by these authors. Partially, the differences observed could also be caused by the presence of diffusion in internal magnetic field gradients, which will influence the T_2 relaxation. Adding the diffusion term to equation (2) accordingly shifts the T_2 pore size distribution function to smaller, unrealistic pore diameter values [Kleinberg, 1999]. Checking the diffusion induced by internal field gradients for the two fine samples, which are more susceptible to be influenced by diffusion, shows that minimum diffusion influence was observed for both the Mix8 and MZ samples for our specific echo time. Therefore, we can conclude that the small observed deviations come from inevitable small errors in the transformation of relaxation distribution functions in PSD cumulative functions.

[20] Comparison of the NMR PSD- T_2 and PSD- T_1 with the pore size distribution functions obtained from mercury intrusion (PSD-Hg) revealed a similar distribution shape for each material. The Hg intrusion measurements provide pore diameter values that are very close to the NMR measurements for sandy samples FH31 and W3. This is most probably due to the fact that these samples were used as sieved materials that were packed at the same packing density for both methods. The differences observed for the sandy materials stem from the fact that the mercury intrusion method is quite limited when materials with relatively large pores are measured. For example, if we assume that pores of 360 μ m or larger can be filled with mercury intrusion at a contact angle of 135°, this implies that the sample is located less than 3 mm below the surface of the mercury in the penetrometer [Micromeritics, 2010]. Otherwise some of the 360 μ m pores are already filled and their volumes accounted for the next pressure step when the remaining pores of 360 μ m are filled. This concludes in an underestimation of pore volume for the given size class. Also, for sieved materials the mercury pressure cannot be extensively increased since high pressure will push the material onto the sides of the sample cup, overestimating the small pores. The Mix8 and MZ samples have been used as a conglomerate to determine the PSD-Hg, which allows us to apply higher mercury pressure, leading to a better estimation of the fine pores. Because of the limitations of our system, the highest pressure applied was 31.7 MPa, which, according to Washburn's equation (equation (4)), will estimate pores no smaller than 0.05 μ m. The differences observed in the Mix8 sample could be due to some differences between the packing density for the NMR measurements and the conglomerate packing density that was used for the Hg intrusion or due to the assumptions made in the calculation of ρ_2 and ρ_1 parameters. In our study, we assumed a homogeneous distribution of the paramagnetic centers, and one average surface relaxivity parameter was calculated for each sample. Jaeger et al. [2009] suggested that for natural soils (e.g., more complex porous systems) the assumption of a homogeneous distribution of an average value of the surface relaxivity parameter is an ideal case. The reason for this is that the shape of the distribution function is strongly affected by the soil texture, and two surface relaxivity parameters (one for micropores and one for mesopores) obtained from NMR data after calibration at two different matric potentials are more convenient when transforming the relaxation time distribution into pore size distribution. This approach is reliable as long as the distributions are clearly bimodal at all saturations so that the distribution modes represent the pore size classes (soil texture) and not other additional effects such as diffusion. Nevertheless, PSD-Hg and PSD- T_2 measured nearly identical pore diameters in the fine pore range. For the MZ sample, the differences observed between PSD-Hg distribution and PSD- T_2 and PSD- T_1 distributions can be due to several facts, such as (1) the sample for NMR measurement was sieved and packed, whereby the sample for mercury intrusion was still in its natural state with smaller aggregates; therefore, large pore structures within the aggregates can still be detected with mercury intrusion, and they shift the PSD-Hg slightly to higher pore diameter values; and (2) PSD- T_1 and PSD- T_2 underestimate the pore diameters because of the bound clay water relaxivity or because of relaxation enhanced by clay particles dispersed in large pores [Kleinberg, 1999].

[21] Comparison of NMR PSD- T_2 and PSD- T_1 with the pore size distribution from retention curves (PSD-pF) revealed a slight difference for the FH31 sample. We assume that this difference is due to measurement errors caused by using the pressure plate method to determine water retention curve. It has been previously reported that pressure plates are susceptible to substantial errors at low water potential [Campbell, 1988; Gee et al., 2002; Cresswell et al., 2008]. Bittelli and Flury [2009] have suggested that for potentials less than $-10 \text{ m H}_2\text{O}$, pressure plates provide considerable errors that can seriously affect the fitted hydraulic functions and their parameters. Furthermore, maintaining exact pressure at low steps is crucial for probes with a steep water release curve such as the FH31 sand. Nevertheless, similar differences are also visible for finer sand such as the W3 sample for which the pF was determined by MSO. The difference between PSD- T_2 and PSD-pF for the Mix8 sample is due to the fact that the retention curve was estimated on the basis of a pedotransfer function with its known uncertainties, especially for artificial fine grained soils. It is also due to an inappropriate average value of the surface relaxivity parameter, ρ_2 , which overestimates the pore diameters because the T_2 distribution of this sample has an unresolved bimodal shape [Jaeger et al., 2009]. Nevertheless, PSD- T_1 of this material is nearly identical to PSD-pF. Because of the fact that for the determination of the pF curve, the MZ sample was used as an undisturbed column, and also because of the similarity between the PSD-pF and PSD-Hg for this sample (these measurements provide similar pore size distributions, and the errors in the pressure plate determination of the MZ pF curve can therefore be considered minimal), one can speculate as to which of the reasons described above have a greater influence on the observed differences between the

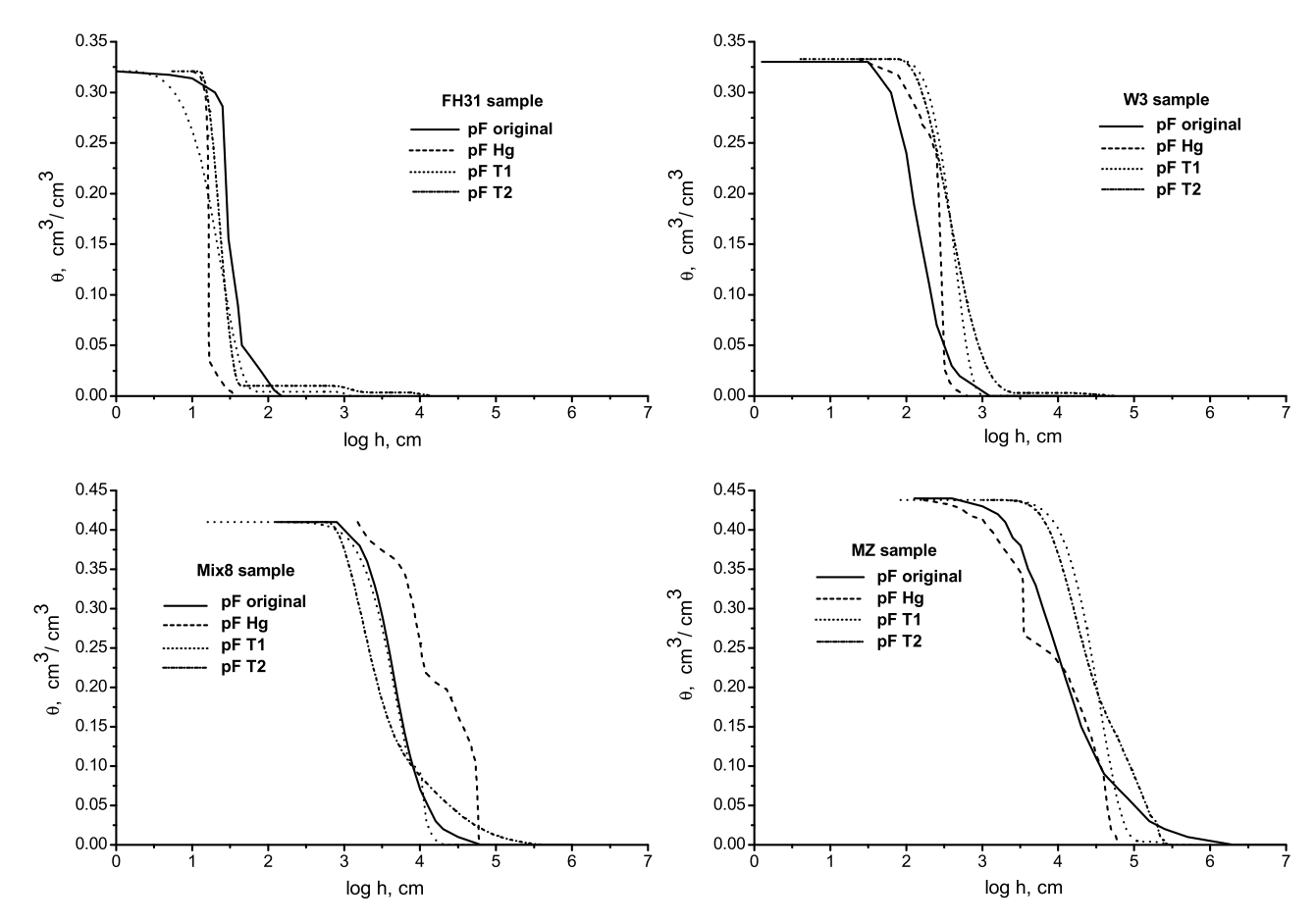


Figure 7. Retention curves (pF) extracted from the different pore size distributions displayed in Figure 6. The retention curve fitting is based on Mualem–van Genuchten parameterization [van Genuchten, 1980].

PSD- T_2 and PSD- T_1 and PSD-pF for MZ soil. If we assume a homogenous distribution of the paramagnetic centers and calculate an average surface relaxivity parameter from both T_1 and T_2 , measurements will overestimate the size of the pores, as Jaeger et al. [2009] have shown. This is due to the bimodal shape of the relaxation distribution functions of this material and explains the differences between PSDs in the small pore range. Furthermore, large pore structures may exist in the undisturbed soil sample used for pF measurements, a fact that explains the differences between PSDs in the macropore range. Finally, PSD- T_1 and PSD- T_2 can underestimate the pore diameters because of the bound clay water relaxivity or because of relaxation enhanced by clay particles dispersed in large pores.

3.5. Hydraulic Properties Estimation

[22] Finally, we analyzed the differences in the calculated retention curves for the four samples and the various measurement techniques because retention characteristics are the main input parameter for numerical simulations for the prognosis of water and solute transport. To do so, the PSD curves were transformed into pF curves on the basis of equation (6). In addition, we fitted the hydraulic parameters of the Mulaemvan Genuchten parameterization [van Genuchten, 1980] using RETC software. Because of the fact that the residual water content, $\theta_{\rm r}$, is often fixed at 0, only the saturated water content, $\theta_{\rm s}$, and the shape parameters α and n were fitted. The calculations

lated retention curves are plotted in Figure 7, and the fitted hydraulic parameters are listed in Table 4.

[23] Again, we can clearly identify the difference in the retention curves of the FH31 sand sample, where the point of first drainage (air entrance) appears earlier than for the NMR-and Hg-derived pF functions, but the overall shape of the curves is not affected. As previously stated, retention curve measurements are often biased and imprecise, especially at low applied pressures. A similar feature was observed for the

Table 4. Soil Hydraulic Properties Extracted Using RETC Software

Sample	Method	$\theta_{\rm s}~{\rm cm}^3/{\rm cm}^3$	$\alpha~{\rm cm}^{-1}$	n
FH31	pressure plates	0.321	0.0330	5.40
	T1	0.310	0.0725	4.19
	T2	0.320	0.0562	5.28
W3	Hg intrusion	0.315	0.0661	12.14
	MSO	0.333	0.0089	2.78
	T1	0.310	0.0076	2.73
	T2	0.340	0.0079	2.73
Mix8	Rosetta	0.410	0.0036	2.66
	T1	0.410	0.0047	2.69
	T2	0.400	0.0050	1.56
	Hg intrusion	0.430	0.0009	2.53
MZ	pressure plates	0.438	0.0071	1.21
	T1	0.434	0.0001	2.95
	T2	0.412	0.0001	1.75
	Hg intrusion	0.430	0.0063	1.58

W3 sample. The curvature itself is not steeper for the NMR or Hg curves, but first drainage occurs later. As previously stated, the differences in the Mix8 pF functions are an artifact of the pedotransfer function, which assumes that natural soils exhibit macroaggregates when a certain percentage of small fractions (silt or clay) are available. The influence of soil structure can additionally be seen in the MZ sample. A slight divergence between NMR, Hg, and pF curves occurs in the wet range, where the pores between macroaggregates and microaggregates were drained. At larger pressures, where soil texture is the only dominant factor in water retention, less divergence was detected.

[24] If we look at the hydraulic parameters, we can see that the saturated water content, θ_s , has been estimated with a relative error of less than 7% for all measurements. The α parameter shows consistent variations between different methods. Nevertheless, the values are in the range of values reported in the literature for similar samples [Schaap et al., 2001]. The most pronounced differences can be observed in the *n* parameter, which describes the slope of the water retention curve. From Table 4 and Figure 7, it can be clearly seen that even for large variations of n (n ranges from 4.19 to 12.14 within FH31 sample), the slope of the calculated pF curves is almost identical within the same sample. This is most probably due to the insensitivity of the water retention function to high values of n. This leads to the conclusion that slight errors in the measurements estimating the slope will lead to extremely large changes in the resulting nparameter.

4. Conclusions

[25] To summarize the findings reported here, we have shown that each measurement technique agrees with the others satisfactorily within one order of magnitude. We observed differences between the techniques, irrespective of whether we focused on the mean pore diameter, pore size distribution, retention curve, or hydraulic parameters. The most interesting finding is that the results of each method do not overestimate or underestimate the results of the other methods. Therefore, it appears that each method is appropriate, within its own limitations, for determining pore size distribution with a strong dependence on the sample characteristics.

[26] If mercury intrusion is applied to loose materials, then the mercury pressure must be carefully limited so that the material is not pushed onto the sample walls leading to unrealistically small values of the pore diameters. Hysteresis effects are always present and could have a major influence when retention data (basically drainage curves) are compared with mercury intrusion data (mostly imbibitions curves). Even the repetition of a measurement on the same sample does not lead to the same retention curve (pressure plate or multistep outflow data), as Mous [1993], Hollenbeck and Jensen [1998], and Weihermüller et al. [2009] have shown in their work. Furthermore, for both mercury intrusion and retention function measurements, the sample preparation (sieving and packing) and maintaining intrusion/extrusion equilibration after each application of pressure are crucial factors.

[27] The determination of pore size distributions by NMR relaxometry has its own drawbacks. First, the diffusion in induced magnetic field gradients can shorten transverse

relaxation times (T_2) . This must be checked and can be minimized by choosing sufficiently small echo times or by measuring longitudinal relaxation (T_1) . Second, diffusion in internal gradients may affect different modes of a multimodal relaxation time distribution function in a different way. The detailed investigation of such phenomena exceeds the framework of this paper but is an important topic for the future. Third, one must be aware that the derivation of PSD is always a scaling procedure which requires independent determination of the average specific surface area. This is usually done using the BET method. Here, large clay contents of a sample can lead to huge S/V ratios, and the derived surface relaxivity parameters, when combined with the average relaxation rates, will have very low values. The reason is that the relaxation times are controlled by the pore sizes and surface relaxivity, but the average S/V is controlled by the internal surface area of the clay. Fourth, the assumption of the homogeneous distribution of pores and paramagnetic centers and the calculation of an average surface relaxivity parameter, especially for a multimodal relaxation time distribution function, leads to an overestimation of the large pores. All these issues, together with the necessary simplification of pore shape and geometry, can deviate the calculated pore size distribution from the real one.

[28] Nevertheless, our study showed that NMR relaxometry can develop as a quick alternative for the estimation of pore size distribution, retention curves, and hydraulic properties. The major advantage of NMR in comparison with classical methods is the short measurement time. This would allow the analysis of large quantities of samples as required to characterize a field or catchment-scale hydraulic properties, which are necessary for risk assessment (e.g., flood forecasting) and management (e.g., fertilization and pest control).

[29] Acknowledgments. Many thanks to Mathieu Javaux and Guido Rentmeesters from UCL, Belgium, for access to and help with Hg intrusion measurements; the DFG (project PO 746/2-1) for financial support; Peter Blümler and Normen Hermes (FZ Juelich) for help with the low-field setup; Anke Langen and Benedikt Scharnagl (FZ Juelich, ICG4) for various retention function measurements; and Claudia Walraf for BET measurements. The reviewers of the paper are also acknowledged for their useful comments and suggestions, which greatly helped us understand and interpret our measurements.

References

Amin, M. H. G., K. S. Richards, R. J. Chorley, S. J. Gibbs, T. A. Carpenter, and L. D. Hall (1996), Studies of soil-water transport by MRI, *Magn. Reson. Imaging*, 14, 879–882.

Barrie, P. J. (2000), Characterization of porous media using NMR methods, Annu. Rep. NMR Spectrosc., 41, 265–278.

Bittelli, M., and M. Flury (2009), Errors in water retention curves determined with pressure plates, Soil Sci. Soc. Am. J., 73, 1453–1460.

Brownstein, K. R., and C. E. Tarr (1977), Spin-lattice relaxation in a system governed by diffusion, J. Magn. Reson., 26, 17–24.

Brownstein, K. R., and C. E. Tarr (1979), Importance of classical diffusion in NMR studies of water in biological cells, *Phys. Rev. A*, 6, 2446–2453.

Brunauer, S., P. H. Emmett, and E. Teller (1938), Adsorption of gases in multimolecular layers, J. Am. Chem. Soc., 60, 309–319.

Campbell, G. S. (1988), Soil water potential measurement: An overview, Irrig. Sci., 9, 265–273.

Carr, H. Y., and E. M. Purcell (1954), Effects of diffusion on free precession in nuclearmagnetic resonance experiments, *Phys. Rev.*, 94, 630–638.

Chelcea, R. I., R. Fechete, E. Culea, D. E. Demco, and B. Blümich (2009), Distributions of transverse relaxation times for soft-solids measured

- in strongly inhomogeneous magnetic fields, J. Magn. Reson., 196, 178-190.
- Cresswell, H. P., T. W. Green, and N. J. McKenzie (2008), The adequacy of pressure plate apparatus for determining soil water retention, *Soil Sci. Soc. Am. J.*, 72, 41–49.
- D'Hollander, E. H. (1979), Estimation of the pore size distribution from the moisture characteristic, *Water Resour. Res.*, 15, 107–112.
- Gee, G. W., A. L. Ward, Z. F. Zhang, G. S. Campbell, and J. Mathison (2002), The influence of hydraulic nonequilibrium on pressure plate data, *Vadose Zone J.*, 1, 172–178.
- Hall, L. D., M. H. G. Amin, E. Dougherty, M. Sanda, J. Votrubova, K. S. Richards, R. J. Chorley, and M. Cislerova (1997), MR properties of water in saturated soils and resulting loss of MRI signal in water content detection at 2 tesla, *Geoderma*, 80, 431–448.
- Hedberg, S. A., R. J. Knight, A. L. MacKay, and K. P. Whittall (1993), The use of nuclear magnetic resonance for studying and detecting hydrocarbon contaminants in porous rocks, *Water Resour. Res.*, 29, 1163–1170.
- Herrmann, K. H., A. Pohlmeier, A. Wiese, N. J. Shah, O. Nitzsche, and H. Vereecken (2002), Three-dimensional nickel ion transport through porous media using magnetic resonance imaging, *J. Environ. Qual.*, 31, 506–514.
- Hinedi, Z. R., A. C. Chang, and M. A. Anderson (1997), Quantification of microporosity by nuclear magnetic resonance relaxation of water imbibed in porous media, *Water Resour. Res.*, 12, 2697–2704.
- Hollenbeck, K. J., and K. H. Jensen (1998), Experimental evidence of randomness and nonuniqueness in unsaturated outflow experiments designed for hydraulic parameter estimation, *Water Resour. Res.*, 34, 595–602.
- Hürlimann, M. D., and D. D. Griffin (2000), Spin dynamics of Carr-Purcell-Meiboom-Gill-like sequences in grossly inhomogeneous B_0 and B_1 fields and application to NMR well logging, *J. Magn. Reson.*, 143, 120–135.
- Jaeger, F., S. Bowe, H. van As, and G. E. Schaumann (2009), Evaluation of ¹H NMR relaxometry for the assessment of pore size distribution in soil samples, Eur. J. Soil Sci., 60, 1052–1064.
- Jury, W. A., and R. Horton (2004), Soil Physics, 6th ed., John Wiley, Hoboken, N. J.
- Kasteel, R., T. Pütz, and H. Vereecken (2007), An experimental and numerical study on flow and transport in a field soil using zero-tension lysimeters and suction plates, *Eur. J. Soil Sci.*, 58(3), 632–645.
- Keating, K., and R. Knight (2007), A laboratory study to determine the effect of iron oxides on proton NMR measurements, *Geophysics*, 1, E27–E32.
- Kleinberg, R. L. (1994), Pore size distributions, pore coupling, and transverse relaxation spectra of porous rocks, *Magn. Reson. Imaging*, 12, 271–274.
- Kleinberg, R. L. (1996), Utility of NMR T_2 distributions, connection with capillary pressure, clay effect, and determination of the surface relaxivity parameter ρ_2 , Magn. Reson. Imaging, 14, 761–767.
- Kleinberg, R. L. (1999), Nuclear magnetic resonance, in Experimental Methods in the Physical Sciences, vol. 35, Methods in the Physics of Porous Media, edited by P.-Z. Wong, pp. 337–377, Academic, San Diego, Calif.
- Kleinberg, R. L., and M. A. Horsfield (1990), Transverse relaxation processes in porous sedimentary rock, *J. Magn. Reson.*, 88, 9–19.
- Kosugi, K. (1994), Three-parameter lognormal distribution model for soil water retention, *Water Resour. Res.*, 30, 891–901.
- Kosugi, K. (1996), Lognormal distribution model for unsaturated soil hydraulic properties, *Water Resour. Res.*, 32, 2697–2703.
- Latour, L. L., R. L. Kleinberg, P. P. Mitra, and C. H. Sotak (1995), Pore size distributions and tortuosity in heterogeneous porous media, *J. Magn. Reson.*, 112, 83–91.
- Meiboom, S., and D. Gill (1958), Modified spin-echo method for measuring nuclear relaxation times, Rev. Sci. Instrum., 29, 688-691.
- Micromeritics (2010), A few facts pertaining to the low pressure performance, technical note, Norcross, Ga. (Available at http://www.micromeritics.com)
- Mous, S. L. J. (1993), Identification of the movement of water in unsaturated soils: The problem of identifiability of the model, *J. Hydrol.*, 143, 153–167.

- Mualem, Y. (1976), A new model for predicting the hydraulic conductivity of unsaturated porous media, *Water Resour. Res.*, 12, 593–622.
- Oswald, S., W. Kinzelbach, A. Greiner, and G. Brix (1997), Observing of flow and transport processes in artificial porous media via magnetic resonance imaging in three dimensions, *Geoderma*, 80, 417–429.
- Pohlmeier, A., D. van Dusschoten, L. Weihermüller, U. Schurr, and H. Vereecken (2008), Imaging water fluxes in porous media by magnetic resonance imaging using D₂O as a tracer, *Magn. Reson. Imaging*, 27, 285–292.
- Pohlmeier, A., S. Haber-Pohlmeier, and S. Stapf (2009), A fast field cycling nuclear magnetic resonance relaxometry study of natural soils, *Vadose Zone J.*, 8, 735–742.
- Raich, H., and P. Blümler (2004), Design and construction of a dipolar Halbach array with a homogeneous field from identical bar magnets: NMR Mandhalas, Concepts Magn. Reson., Part B, 23B, 16–25.
- Schaap, M. G., F. J. Leij, and M. T. van Genuchten (2001), Rosetta: A computer program for estimating soil hydraulic parameters with hierarchical pedotransfer functions, *J. Hydrol.*, 251, 163–176.
- Schaumann, G. E., E. Hobley, J. Hurraß, and W. Rotard (2005), H-NMR relaxometry to monitor wetting and swelling kinetics in high-organic matter soils, *Plant Soil*, 275, 1–20.
- Song, Y. Q., L. Venkataramanan, M. D. Hürlimann, M. Flaum, P. Frulla, and C. Straley (2002), T_1 – T_2 correlation spectra obtained using a fast two-dimensional Laplace inversion, *J. Magn. Reson.*, 154, 261–268.
- Stingaciu, L. R., A. Pohlmeier, P. Blümler, L. Weihermüller, D. van Dusschoten, S. Stapf, and H. Vereecken (2009), Characterization of unsaturated porous media by high-field and low-field NMR relaxometry, Water Resour. Res., 45, W08412, doi:10.1029/2008WR007459.
- Straley, C., D. Rossini, H. Vinegar, P. Tutunjian, and C. Morriss (1997), Core analysis by low-field NMR, Log Anal., 38, 43–56.
- Tuller, M., and D. Or (2001), Hydraulic conductivity of variably saturated porous media: Film and corner flow in angular pore space, *Water Resour. Res.*, 37, 1257–1276.
- Tuller, M., D. Or, and L. M. Dudley (1999), Adsorption and capillary condensation in porous media: Liquid retention and interfacial configurations in angular pores, *Water Resour. Res.*, 35, 1949–1964.
- Van As, H., and D. van Dusschoten (1997), NMR imaging of transport processes in microporous systems, Geoderma, 80, 389–403.
- van Genuchten, M. T. (1980), A closed-form equation for predicting the hydraulic conductivity of unsaturated soils, *Soil Sci. Soc. Am. J.*, 44, 807–808
- Vogel, H. J. (2000), A numerical experiment on pore size, pore connectivity, water retention, permeability, and solute transport using network models, Eur. J. Soil Sci., 51, 99–105.
- Votrubová, J., M. Šanda, M. Císlerová, M. H. G. Amin, and L. D. Hall (2000), The relationships between MR parameters and the content of water in packed samples of two soils, *Geoderma*, 95, 267–282.
- Washburn, E. W. (1921), The dynamics of capillary flow, *Phys. Rev.*, 17, 273–283.
- Webb, A. P. (2001), An introduction to the physical characterization of materials by mercury intrusion porosimetry with emphasis on reduction and presentation of experimental data, technical article, Micromeritics, Norcross, Ga.
- Weihermüller, L., J. A. Huisman, A. Graf, M. Herbst, and J.-M. Sequaris (2009), Multistep outflow experiments to determine soil physical and carbon dioxide production parameters, *Vadose Zone J.*, 8, 772–782.
- S. Haber-Pohlmeier, Macromolecular Chemistry Department, RWTH Aachen University, D-52074, Aachen, Germany.
- A. Pohlmeier, L. R. Stingaciu, H. Vereecken, and L. Weihermüller, Agrosphere Institute, ICG-4, Forschungszentrum Jülich, D-52425 Jülich, Germany. (l.stingaciu@fz-juelich.de)
- S. Stapf, Department of Technical Physics II, Ilmenau University of Technology, D-98684 Ilmenau, Germany.